



Effect of Shot Peening on Oxidation and Precipitation in Inconel 718

S. Barella¹ · M. Belfi¹ · I. Fernández-Pariente² · A. Gruttadauria¹ · D. Ripamonti³ · L. B. Peral²

Received: 5 April 2022 / Revised: 10 May 2023 / Accepted: 26 May 2023 /

Published online: 16 June 2023

© The Author(s) 2023

Abstract

In this study, the effect of the surface state on the behaviour of Inconel 718 alloy exposed to 640 °C and 700 °C environments for times varying between one and one hundred hours was investigated. In particular, the focus was set on the evolution of oxidation and precipitation phenomena during thermal exposure. Three surface states were considered: two generated through shot peening treatments featuring different coverage levels, while the third condition is a non-peened one. Shot peening treatments modify the surface condition and introduce higher residual stresses and microhardness values than in the non-treated condition. The morphology of the oxides appears to be different depending on the condition observed. Regarding the kinetics, over time the oxidation process follows a parabolic trend and appears to be influenced by the surface state; in particular, severe shot peening treatment is characterized by the highest intensity of the phenomenon. However, the order of magnitude of the weight gains measured suggests that the observed variations can be neglected, and that the positive effect of shot peening can be exploited without introducing oxidation problems. From the point of view of the microstructural evolution, an increase in the coarsening kinetics of γ'' phase was observed in the shot peened layer.

Keywords Superalloys · Shot peening · Oxidation · Precipitation · Inconel 718

✉ M. Belfi
marco.belfi@polimi.it

¹ Politecnico di Milano, Via Privata Giuseppe La Masa, 1, 20156 Milano, Italy

² Universidad de Oviedo, Campus de Gijón, 33203 Gijón, Spain

³ CNR - ICMATE, Via Roberto Cozzi, 56, 20126 Milano, Italy

Introduction

The request for high energy production in recent years has led to the need of an increase in the performance of the machines that are involved in the power generation processes. This improvement in the technology has been achieved often reaching higher cycle temperatures, setting a new target for the components that are stressed in this condition. In this scenario, nickel alloys are widely used in the energy production industry because of their unique combination of good mechanical properties and high temperature resistance. Multiple studies have been performed to design the correct alloy in relation to the application required, taking into account the particular operating conditions and the properties called for. Inconel 718, in particular, is a widely used grade for multiple applications, such as turbine discs, blades and combustion chambers, as it features good mechanical properties both at high and cryogenic temperatures, as well as oxidation resistance [1–5]. Inconel 718 microstructure is characterized by a γ matrix mainly composed of nickel, chromium and iron. Inside this matrix, the main strengthening phases for the alloy $\gamma'(Ni_3(Al;Ti))$ and in particular $\gamma''(Ni_3Nb)$ are precipitated. The stability of these phases for temperatures up to 650 °C is the reason why this alloy is used in this range of temperatures. For higher-temperature values indeed, γ'' starts overageing and transforming in the δ phase, featuring the same composition but an orthorhombic morphology. The presence of such a phase does not increase the mechanical properties of the alloy because of its different morphology, but instead has a harmful effect since it leads to a loss of hardenability because its generation occurs with a depletion of γ'' , and moreover, increases in hot cracking problems have been observed. However, studies have discovered that its presence can have positive effects too, since it was reported that it can control the grain size and block grain boundary sliding; if the morphology and quantity are correct, the δ phase is capable of enhancing the resistance to grain boundary creep fracture and to limit grain growth during solution treatments [6]. Another phase which can be present in Inconel 718 is a hexagonally close packed phase called Laves phase $(Ni;Cr;Fe)_2(Nb;Mo;Ti)$, which is a brittle intermetallic compound typically formed due to segregation in the interdendritic zones that occurs during welding processes where the concentrations of these elements are increased by segregation [7]. In addition, the presence of carbides controls the alloy's resistance, since their fine precipitation in the matrix influences the final hardness, while their presence in the correct shape and quantity at the grain boundaries is linked to creep properties as it controls grain size [8]. It should be noticed that both niobium and titanium carbides are usually present [9], and their origins can be multiple: some primary ones are created through heat treatments, while other ones are produced during thermal exposure. Carbides present in the microstructure can have various compositions (in particular $M_{23}C_6$ and MC).

As components used in energy systems are often subjected to time-varying stresses, fatigue tasks are introduced for manufacturers: surface treatments such as shot peening can be implemented on various materials, which, by introducing compressive residual stresses into the surface layer of the material [10], can enhance the components' wear and fatigue behaviour [11–13]. Indeed, multiple studies have

shown that fatigue life can be increased for Inconel 718 by applying surface enhancing treatments, even taking into account the lessening of the stresses due to the thermal exposure [14–16]. Moreover, another damaging phenomenon that occurs in high-temperature environments is oxidation, which consists of the progressive generation of oxide scales on the external surface of the material [17, 18]; this situation can be harmful because depending on the amount, the morphology and in particular the adherence of such oxide scales, it can lead to damage and failure of the components [19], as some sites prone to crack initiation can be introduced on the surface.

However, roughness and other surface features such as the microstructure in the surface layer are generally modified by these treatments. As it was found out for multiple alloys, oxidation is closely related to the surface conditions of the material [20–24], so every variation introduced influences the development of this phenomenon, which in some cases can be dangerous for the strength of the material itself. Moreover, the combination of a compressed layer and thermal exposure can enhance metallurgical phenomena such as the precipitation of secondary phases [25, 26], the presence of which is the main strengthening mechanism for the material and hence has a strong influence on its final properties. As a consequence, the application of surface treatments, such as shot peening, should be carefully studied taking into account all their effects, both on fatigue life and on oxidation and precipitation. Although the positive effect on fatigue life of shot peening is well-known, in the operating conditions of these alloys, this treatment can introduce modifications in the phenomena indicated previously, which may endanger the integrity of the material. Indeed, variations in precipitation can modify the mechanical properties in the affected zone, while an oxidation process that is too intense, or in which the scales are not very compact, is capable of introducing sensitive zones in the material which are more prone to crack initiation.

Therefore, this study focuses on characterization of the variations in the surface state generated by treatments that are commonly used in industry such as shot peening, and its consequent effect on the evolution over time of phenomena such as oxidation and precipitation during the first phases of high-temperature exposure. It does so to establish whether applying these treatments, with the aim of enhancing fatigue life, can introduce problems in these other phenomena.

Materials and Methods

The material used is an Inconel 718 alloy (UNS 7718), given in a forged condition at a 5:1 ratio, the composition of which conforms to ASTM B637 standard.

A heat treatment made up of solubilization (980 °C, 1 h, water quenching) and double ageing treatment (720 °C and 620 °C, 8 h each, followed by an air cooling) was carried out.

The microstructure was observed through a Nikon Eclipse MA200 optical microscope and a JEOL JSM-5600 SEM which was used in addition to perform EDS analysis. Specimens were etched with the following mixture: 50 ml *HCl* + 10 ml *NO₃H* + 2 ml *HF* + 38 ml *H₂O*.

Table 1 Selected fixed parameters for shot peening treatments

| Proyectil | Pressure | Almen Intensity | Head height |
|--------------|----------|-----------------|-------------|
| Zirshot y300 | 4 (bar) | 10 (A) | 23 (cm) |

Table 2 Relationship between processing time and coverage level

| Treatment | Coverage (%) | Time (s) |
|--------------|--------------|----------|
| Conventional | 98 | 5 |
| Severe | 5000 | 250 |

Shot peening treatments were carried out using a Guyson EUROBLAST 4PF SYSTEM machine equipped with Zirshot y300 spheres [27]. Two shot peening treatments featured by different coverage levels were designed, as shown in Table 1. In particular, the conventional treatment is featured by a 100% coverage level, while the treatment designed and termed severe refers to higher levels of coverage. In particular, in this study, a coverage level of 5000 % was chosen for the severe treatment.

The time necessary to achieve a desired coverage level has been computed according to Avrami's law:

$$C(\%) = 100 \cdot (1 - e^{-ARt})$$

The AR factor is called coverage rhythm factor and is the product of the area of each impression (A) and the uniform rate of creation of impressions (R). This AR factor is constant for treatments using the same spheres, Almen Intensity and material, and it was calculated by applying shot peening to a sample for one second. Coverage has been estimated by means of images analysis. The factor obtained is then used to determine time to achieve a desired coverage level [28]. It should be noted that the time for the severe condition was determined assuming that after the complete saturation, coverage follows a linear trend over time. Results are summarized in Table 2.

The characterization of shot peening effects was done through different technologies. X-ray diffraction was used to characterize the residual stresses introduced, by means of an Xstress 3000 diffractometer. The residual stress field induced by the applied shot peening treatments was measured by means of X-ray diffraction technique, using a Stress-tech 3000-G3R X-ray diffractometer. The K_α chromium wave length (0.2291 nm) was employed onto the 200 austenite planes under a 2θ angle of 128.8°. The residual stress was determined using the $\sin^2\psi$ technique by means of Eq. [29]:

$$\sigma_\phi = (E/(1 + \nu))_{(hkl)}(1/d\phi_{0(hkl)})(\partial d\phi_{\psi(hkl)}/\partial \sin^2\psi)$$

where 'E' and ' ν ' are the elastic modulus and Poisson coefficient of the Inconel 718 in the measured crystallographic plane, taken as 200000 MPa and 0.3, respectively; 'd' is the interplanar distance of the selected diffraction plane (hkl), ' ψ ' the tilt angle and ' ϕ ' the angle in the sample plane. The detection of the diffraction peak was carried out at five positions of the tilt angle, between -45° and +45°, along three rotations of 0°, 45°, and 45° and using an exposure time of 20 s in each position. In

order to remove material and measure the stress in depth, an electropolishing technique was employed, using 94% CH_3COOH + 6% $HClO_4$ as the reactant solution. The results of the in-depth residual stress measurements were corrected by using the method described in [30]. Microhardness profiles were performed with a BUEHLER MAT 419 C tester machine, with 200 gf precharge and 10 (s) dwell time, following ISO 6507 norm. Measures were taken at 25 μm steps. Three different profiles were measured for each condition. Lastly, roughness measurements were taken with a Mahr MarSurf M300 following the ISO 4287 norm.

Specimens were subjected to thermal exposure in air atmosphere meant to simulate the operating conditions that the material undergoes in its service life. Two different temperature levels (640 °C and 700 °C) were selected as the material is commonly used for applications in this range of temperatures. Different exposure times (1, 10, 50, 100 h) were tested in order to investigate the evolution of multiple phenomena step by step over time, such as oxidation and precipitation in the first stages of high temperature maintenance.

Observation of the oxide scales formed during the thermal exposure, investigation on the microstructural evolution and EDS analyses were performed through Zeiss Sigma 500 SEM. Weight gain analysis was done using a Scatec SBC22 scale with a 0.01 mg sensitivity; a different sample for each condition was tested. Image handling was accomplished using NIH ImageJ software.

Results and Discussion

Material was in a forged condition. Optical microscopy shows a nonuniform precipitation (Fig. 1a); this is not a favourable condition as chemical and physical anisotropy could introduce differences in the properties of different zones of the material.

After the application of a standard heat treatment composed of solubilization and ageing, in order to achieve a structure in which strengthening phases γ' and γ'' have precipitated in the matrix, the microstructure appeared to be more homogeneous and composed of approximately equiaxed grains, with a balanced carbides dispersion throughout all the material (Fig. 1b). Moreover, the presence of niobium

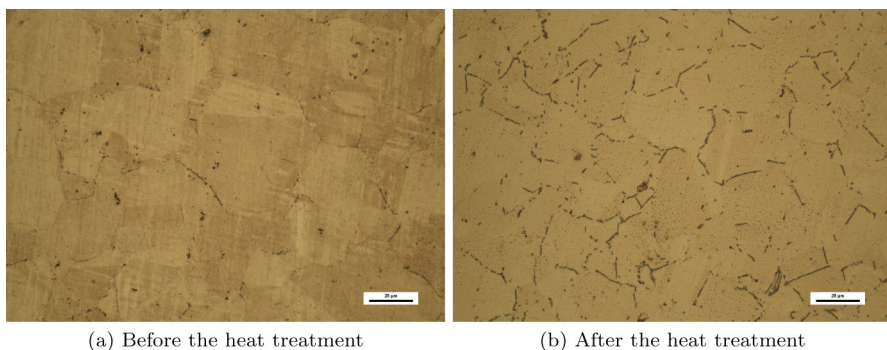


Fig. 1 Optical microscopy of base material, before and after the heat treatment

and titanium carbides should be pointed out, which are finely dispersed both at the boundaries and inside the grains; this homogeneity and fine dispersion is looked for in the material in order to achieve the desired mechanical properties. The presence of some δ phase at the grain boundaries in the typical platelets shape can be observed.

Microstructure results modified by the different surface treatments; in particular, the outermost layer of the severe shot peened material features grains that have been intensively deformed, and are widely elongated in the horizontal direction; this phenomenon decreases moving towards the bulk material, where grains are more equiaxed (Fig. 2b). This is coherent with the application of a surface treatment; its effect is expected to be high in the outermost layer and then to decrease in the inner part of the material. On the other hand, the material subjected to the conventional treatment did not show such an intense modification in the shape of the grains, which are characterized by the presence of slip bands related to the onset of a deformation process (Fig. 2a), as was observed previously for this material by Klotz et al. [14]. It should be noted that the severe shot peened specimens show a deeper modified layer than the conventional shot peened ones; depending on the process parameters, the depth of the influenced layer can differ, but after a certain distance from the surface, the material was found to not be modified by the treatment. Thus, the variations induced in its properties are also expected to be limited to the superficial layer impacted by the treatment.

Coherently with these observations, the same trend was detected in the microhardness profiles. Indeed, microhardness appears to be increased by the application of shot peening treatments; in particular, as expected for a surface treatment, the effect reduces moving towards the bulk material until it reaches the value of the non-treated material (470 HV) asymptotically. Figure 3 shows the Vickers microhardness evolution on the cross section of the shot-peened samples: base material, conventional shot peening, and severe shot peening series. After applying shot peening treatments, a notable increment in the hardness level in the upper layer of the samples (around 200–250 μm) is appreciable in shot peened series. The increment in hardness is directly related with the amount of energy induced onto the material, increasing with coverage level [10, 31,

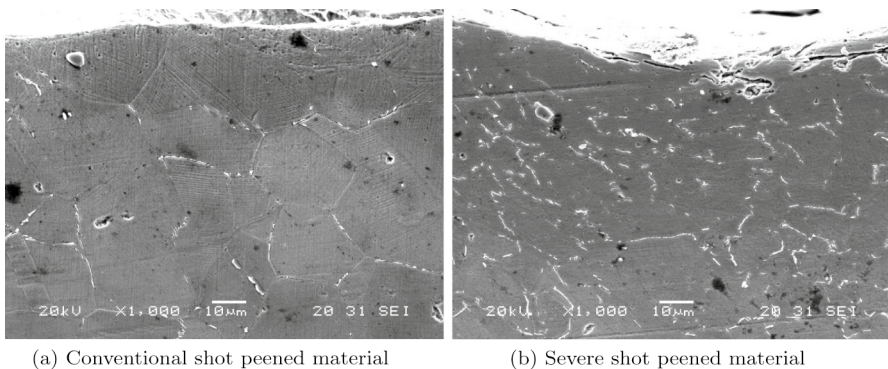


Fig. 2 Microstructural modifications in the outermost layer of peened specimens

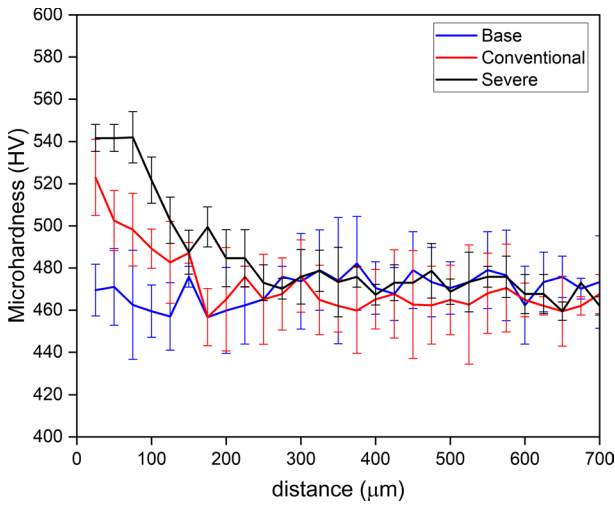


Fig. 3 Microhardness comparison in the different conditions

32]. This fact can be associated to the grain refinement and increased dislocation density caused by the plastic deformation induced by means of the shot peening treatments, as confirmed in [33]. It should be noted that on comparing the effect of the two different treatments, it can be observed that severe shot peening introduces higher microhardness values (up to 543 HV) and a thicker modified layer (up to 250 μm) than the conventional treatment (Fig. 3). The presence of scattering in the data might be related to the presence of multiple secondary phases and carbides in the sample zones, which might cause the dispersion in the measured values. However, in order to minimize this effect and give a better estimation of the microhardness profile, multiple measurements were taken, and the overall curve follows the trend expected.

In addition, roughness appears to be increased by the application of the surface treatments: all the parameters taken into account (R_a , R_{max} and R_z) are increased by an order of magnitude by applying shot peening treatment compared to the as-cut condition and in particular the highest roughness values are those introduced by severe shot peening (Table 3).

The characterization of the effect of the surface treatments was concluded with measurement of the residual stresses introduced by the different treatments. A sample subjected to conventional shot peening, and one to severe shot peening were tested; these samples were meant to exemplify the initial condition of the peened samples before the oxidation process. The plots of residual stresses follow the expected trend for

Table 3 Roughness measurements summary

| Roughness parameter (μm) | Ra | Rz | Rmax |
|---------------------------|------|-------|-------|
| Severe shot peening | 3.73 | 21.95 | 27.29 |
| Conventional shot peening | 3.16 | 17.81 | 22.75 |
| Base material | 0.27 | 2.18 | 3.088 |

a shot peened material (Fig. 4); the effect of the treatment decreases moving towards the inner part of the material [34]. The same is true for the residual stresses, which increase for the first tens of micrometres from the surface, even exceeding 1000 MPa in absolute value, and then progressively diminish until 275 μm where it reaches the zero value. It should be noted that both treatments show similar trends, and that the maximum absolute value reached and the depth influenced are quite similar. In addition, this low value for the residual stresses was surprising after the observation of the microstructural modifications that occurred in the severe shot peened specimens, which appeared to be more intense compared to those subjected to the conventional treatment.

The introduction of these different surface states on the same material was expected to cause variations in both oxidation, as the area and the presence of a compressive stress state are reported to have an influence on the kinetics of the process, and in precipitation of secondary phases, as studies have shown an important increase in the phenomenon in the modified layer. The formation of oxide scales appears to be influenced by the different surface conditions introduced by the shot peening treatments, as different morphologies are detected in the three cases (Fig. 5). Oxide scales are generated on severe shot peened specimens in the form of flaky structures that progressively form the oxidized layer. Conventional shot peened specimens show the lowest variations over time regarding the oxidation process, in terms of both the kinetics and the morphologies of the oxides. Indeed, a thin oxide layer is generated in the very first stages of the process, and after that phase, no major differences are detected over time. The variation in the presence of flakes over time seems to suggest that the generation of the layer occurs through the generation of these structures; however, the process seems to be more akin to a passivation phenomenon that occurs in the first steps of the maintenance period, which is followed by a practically null growth of the oxide scale, as proposed by Greene et al. [35]. However, the base material

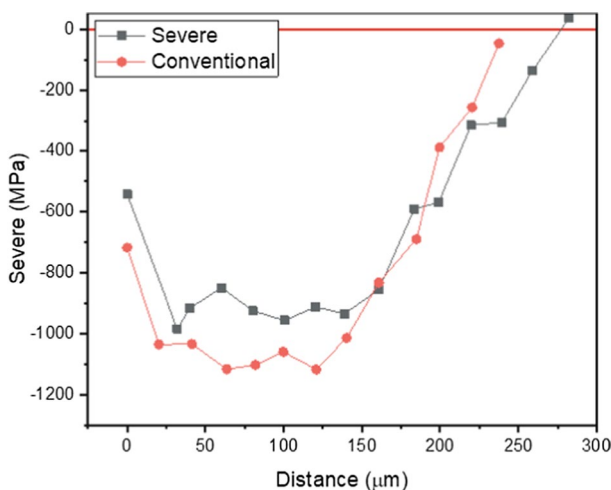


Fig. 4 Residual stresses comparison along the shot peening treatments

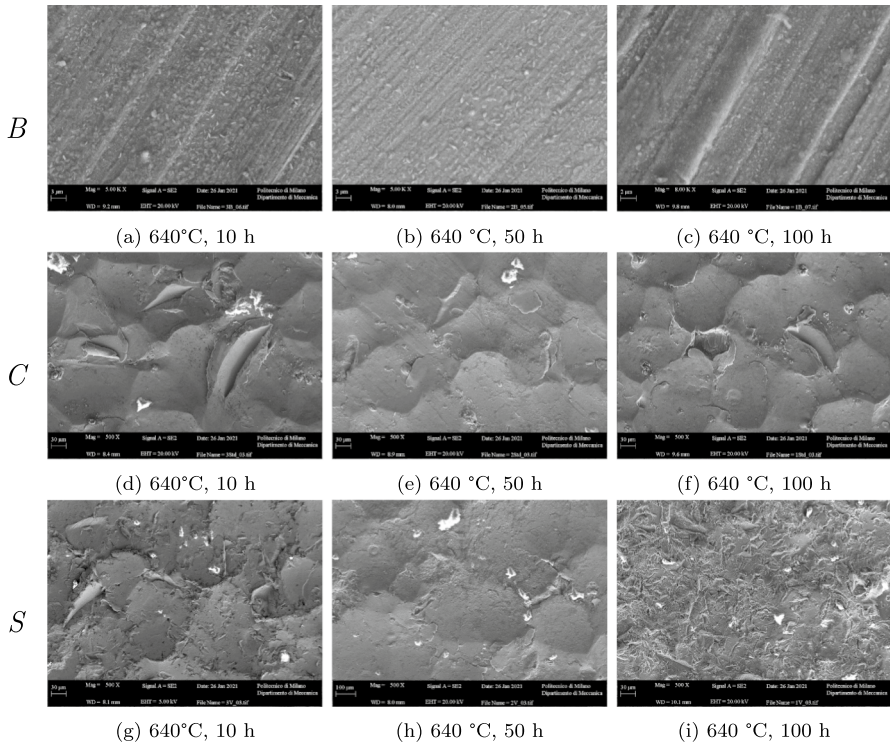


Fig. 5 Surfaces of 640 °C oxidized specimens. Base material (B), Conventional shot peened (C), Severe shot peened (S)

appears to feature the nucleation of needle-shaped particles, which progressively increase in quantity and dimension until they create a compact layer over which the process can restart, generating a new one featuring needle-like structures.

Comparing the 640 °C and 700 °C conditions, one must understand that since the temperature variation selected is quite low, the differences detected are not disruptive. However, it can be noted that in the latter case the kinetics seem to have increased, since the same phenomena happened there earlier; one can note for example that in the base material specimen oxidized for 10 h, the higher temperature environment has enhanced a more compact and uniform formation of the needle-shaped oxides, whereas in the 640 °C case, they are quite sparse. Between these two different temperature levels, no major differences in morphology are observed apart from faster kinetics, and so the same oxidation level is achieved after a shorter time for a higher temperature (Fig. 6). As regards composition, we must point out that in all cases, the oxide scales appear to be mainly composed of chromia (Cr_2O_3) (Table 4).

The main difference observed in the 700 °C thermal exposure is the deposition of chromium rich islands on the specimens subjected to conventional shot peening and especially the non-peened ones for times greater than 50 h, which were

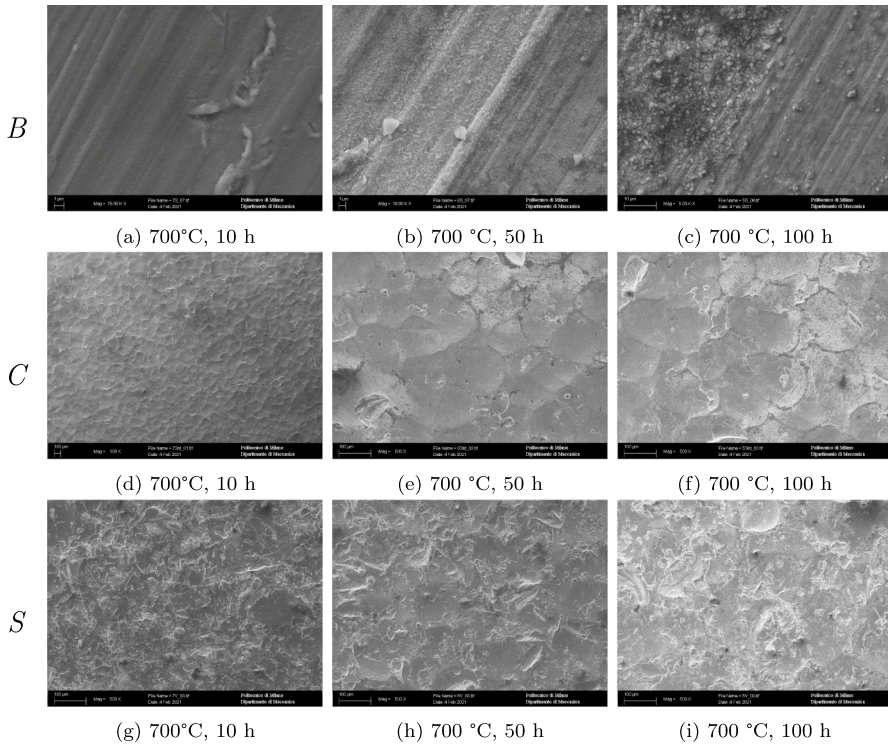


Fig. 6 Surface of 700 °C oxidized specimens. Base material (B), Conventional shot peened (C), Severe shot peened (S)

Table 4 EDS analysis of severe shot peened specimen oxidized at 640°C for 100 h

| Element | Ni | Cr | Fe | O | C | Nb | Mo | Ti | Al |
|---------|------|------|------|------|-----|-----|-----|-----|-----|
| wt% | 41.6 | 20.9 | 16.0 | 10.8 | 4.2 | 2.6 | 1.6 | 1.0 | 0.9 |

not visible in the 640 °C exposed specimens, as shown in Fig. 7; these structures are similar to the ones observed for cyclic oxidation at 750°C by Al-Hatab et al. [36]. It should be pointed out that these structures do not progressively cover the entire surface of the material and in the case of non-peened material they are oriented preferentially in the same direction as the lines resulting from the cutting process, as shown in Fig. 7. Therefore, it has been proposed that the presence of these islands is related to the surface state induced by the cutting process itself, and the severe shot peened ones do not show this behaviour as their surface has been modified in a deeper way.

A simple investigation was carried out to verify this hypothesis; samples were polished and subjected to the same 700 °C thermal exposure for 50 h to observe if the phenomenon occurred even in this condition; in this case, these structures

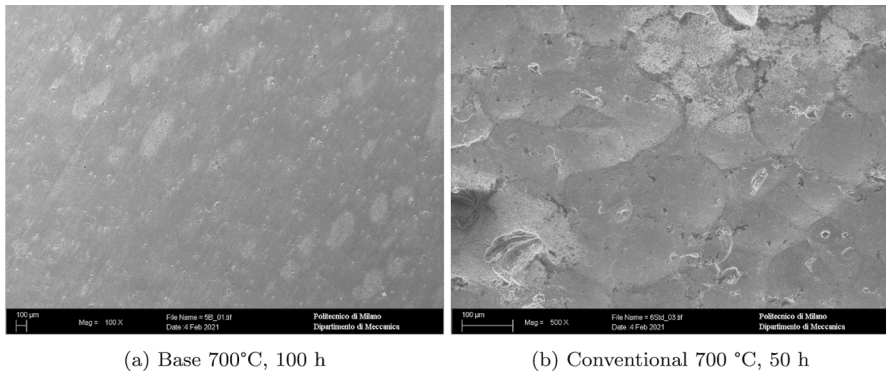
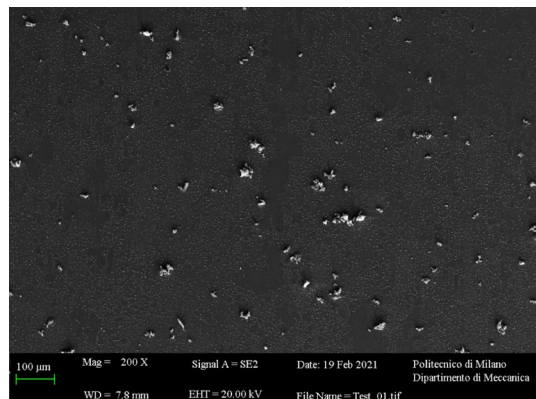


Fig. 7 Chromium rich islands detected after 700 °C exposure

were not detected anymore, so it was concluded that probably the phenomenon is actually linked to a combination of surface state and thermal exposure (Fig. 8).

Oxidation kinetics were evaluated by measuring the weight gain over time; this parameter is capable of giving an idea of the intensity of the oxidation process, as high weight gain values are associated with extensive oxide generation and therefore an intense oxidation process. Inconel 718 was expected to show a parabolic behaviour over time [35], and the values measured (Fig. 9) agree with this hypothesis, as the growth of the oxide scales appears more rapid in the first stages of the thermal exposure while its increased rate slows down progressively over time, following a parabolic trend with highly reduced rate. This result is in agreement with those proposed by Greene et al. who observed for IN718 at 700 °C, a first phase (around 24 h) in which the oxide scales form rapidly and after that follow a parabolic behaviour at a rate so low that is quite immeasurable [35]. These considerations fit with the experimental data discussed here, since the quantities measured in this analysis are so low (lower than 0.06 mg/cm^2 even in the most oxidized condition at 700 °C) that are practically null. Indeed, by comparing these

Fig. 8 Absence of chromium-rich islands in polished specimen, oxidized at 700 °C for 50 h



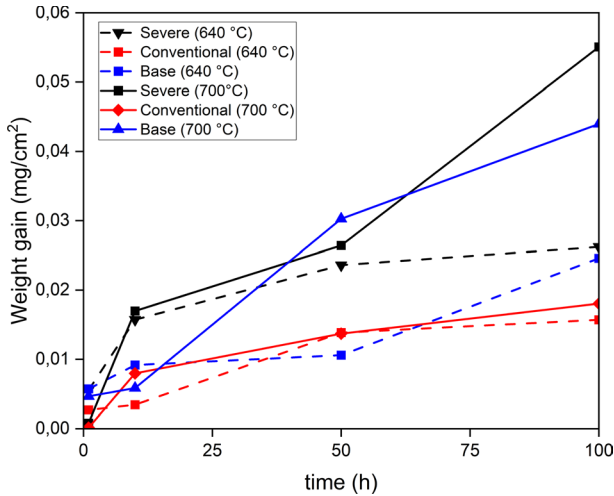


Fig. 9 Weight gain comparison in different conditions

values with those found at higher temperatures in literature [35], one can observe that the weight gains measured in this case are between one and two order of magnitudes lower than those observed and extensively studied in the study at higher temperatures, so that, by comparison, they are too low to be considered. One can observe that severe shot peened specimens feature the highest weight gain both at 640 °C and 700 °C and that kinetics are increased for the same surface state, by increasing the temperature level. However, it should be noted that all the oxidation levels are characterized by very low values: even though the cases show qualitatively different behaviours, the differences in order of magnitude are so low that at a practical level they can be considered negligible. This result is important since one important concern regarding the implementation of shot peening treatments on the material, was the possible increase in the oxidation kinetics, which could lead to the detachment and spalling phenomena that can generate weaker zones in the material: the low magnitudes of the weight gains and the consequent tiny thickness observed suggest that the positive effects of these surface enhancement methods can be exploited without taking into account the possible harmful effects related to the introduction of the higher roughness and the compressive state in the oxidation process.

Cross-sectional analysis was performed to investigate the evolutions that occur during the thermal exposure, in relation to both microstructure and oxidation. One can see that the oxide layer is so thin that is not practically possible to identify an evolution over time; this result is in agreement with the weight gain analysis, which indicated that even if an oxidation process is occurring, the amount of oxides that is formed is so low that their thickness must be particularly tiny. This consideration is valid for all the different surface conditions taken into account in the study; therefore, the analysis focused on the microstructural evolution in the more superficial layer in order to evaluate the presence of differences regarding

the microstructure. We focussed particularly on the precipitation of secondary phases in the peened layer compared to the non-treated one.

Cross-sectional analysis for the shot peened specimens show an interesting evolution in the coarsening kinetics of secondary phases in their outermost layer, which is the one influenced by the treatment. Specimens exhibit the development of small needle like structures, the penetration depth of which increases with exposure time (Fig. 10). It should be noted that these needle-shaped phases increase progressively in size towards the surface, and that their protrusions seem to follow some preferential paths in their in-depth development, which can be related to the presence of grain boundaries. Comparing the result obtained with that found by Cai et al. [37], it was deduced that these phases are probably γ'' ones, whose coarsening kinetics are promoted strongly in the shot peened layer; this precipitation effect may be related to an increased diffusion due to the intense introduction of defects into the outermost layer of the material caused by the surface treatment applied. The observation of this disparity in the precipitation, the behaviour of which seems to vary widely between the surface and the inner part of the material, suggests that the compressive residual state enhances the precipitation of secondary phases in the modified layer. The phenomenon especially starts in the more superficial zone, which experiences the thermal load first, and then moves towards the inner part as the time increases. This leads to the supposition that, for longer exposure times, the layer affected may increase further [38]. This result is consistent with findings by Qin et al. that observed a stress-assisted diffusion which leads to faster γ'' precipitation kinetics [39].

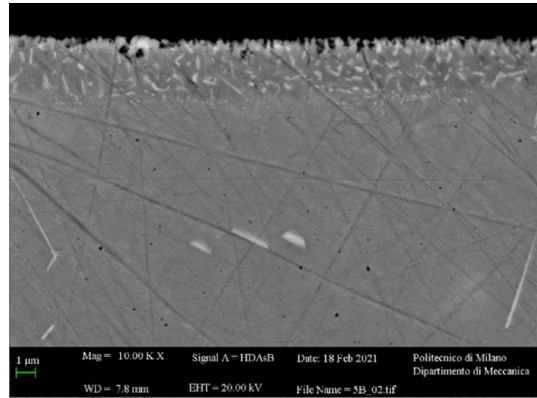
A preliminary investigation has been carried out in order to establish the effect of these modified coarsening kinetics on the properties of the material. Microhardness tests have been performed at a 25 μm distance from the surface and compared with the values measured before the thermal exposure; results are summarized in Table 5. No major differences regarding microhardness were found. However, further analyses are needed in order to better investigate the effect of this phenomenon on the mechanical properties of the surface state, which is a very sensitive area in the operating field.

Conclusions

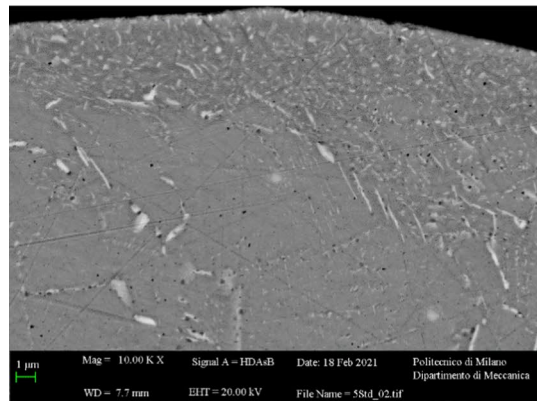
The aim of the study was to evaluate the effect of shot peening treatment on the microstructural evolution and the oxidation process for Inconel 718 during the first stages of thermal exposure.

1. Shot peening treatments induce an increase in the residual stresses trend, surface hardening and roughness.
2. Oxide morphologies are influenced by the different surface states, with the formation of needle shaped oxides on the base material, flakes on the severe shot peened ones, and a more compact and uniform layer for conventional treatment.

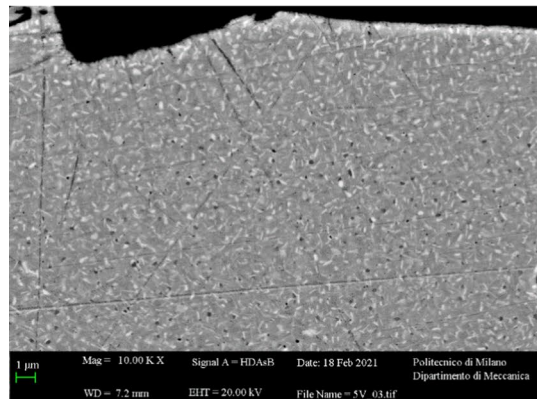
Fig. 10 Cross sections of specimens subjected to 700 °C, 100-h thermal exposure



(a) Base material



(b) Conventional



(c) Severe

- Oxidation kinetics vary between the different conditions; oxidation is more intense for the severe shot peened specimens, while the conventional shot peened ones feature the lowest weight gain.

Table 5 Microhardness comparison at 25 μm from the surface before and after 700°C 100 h thermal exposure

| Treatment | HV (after) | HV (before) |
|---------------------------|------------|-------------|
| Severe shot peening | 546 | 542 |
| Conventional shot peening | 527 | 524 |
| Base material | 475 | 470 |

- Precipitation kinetics differ from those of untreated material; enhanced γ'' coarsening kinetics have been detected in the outermost layer of the specimens, which are faster for higher thermal exposures.
- Specimens subjected to severe shot peening exhibit the deepest modified layer as well as the deepest coarsening area.
- As the order of magnitude of the weight gain is low, it is possible to propose that the variations observed for oxidation are practically negligible; the design and the implementation of shot peening treatments on components that work at high temperature can be performed exploiting their positive features on fatigue life without taking into account the issues regarding oxidation.

Author Contributions All authors reviewed the manuscript

Funding Open access funding provided by Politecnico di Milano within the CRUI-CARE Agreement.

Declarations

Conflict of interest The authors declare no competing interests.

Open Access This article is licensed under a Creative Commons Attribution 4.0 International License, which permits use, sharing, adaptation, distribution and reproduction in any medium or format, as long as you give appropriate credit to the original author(s) and the source, provide a link to the Creative Commons licence, and indicate if changes were made. The images or other third party material in this article are included in the article's Creative Commons licence, unless indicated otherwise in a credit line to the material. If material is not included in the article's Creative Commons licence and your intended use is not permitted by statutory regulation or exceeds the permitted use, you will need to obtain permission directly from the copyright holder. To view a copy of this licence, visit <http://creativecommons.org/licenses/by/4.0/>.

References

- R. C. Reed, *The Superalloys as High-Temperature Materials*, (Cambridge University Press, Cambridge, 2006).
- E. Bernini, *Advances in Gas Turbine Technology*, (InTech, Croatia, 2011).
- T. M. Pollock and S. Tin, Nickel-based superalloys for advanced turbine engines: Chemistry, microstructure, and properties. *Journal of Propulsion and Power* **22**, (2), 361–374 (2006). <https://doi.org/10.2514/1.18239>.
- K. Singh, Advanced materials for land based gas turbines. *Transactions of the Indian Institute of Metals* **67**, 601–615 (2014). <https://doi.org/10.1007/s12666-014-0398-3>.

5. N. Andrzej, K. Krzysztof, S. Jan, R. Paweł, P. Paweł, and M.-N. Grażyna, Development of nickel based superalloys for advanced turbine engines. *Materials Science Forum* **786**, 2491–2496 (2014). <https://doi.org/10.4028/www.scientific.net/MSF.783-786.2491>.
6. S. Azadian, L. Wei, and R. Warren, Delta phase precipitation in Inconel 718. *Materials Characterization* **53**, 7–16 (2004). <https://doi.org/10.1016/j.matchar.2004.07.004>.
7. R. Radhakrishna, The formation and control of Laves phase in superalloy 718 welds. *Journal of Materials Science* **32**, 1977–1984 (1997).
8. C. Kuo, Y. Yang, H. Bor, C. Wei, and C. Tai, Aging effects on the microstructure and creep behavior of Inconel 718 superalloy. *Materials Science and Engineering A* **511**, 289–294 (2009). <https://doi.org/10.1016/j.msea.2008.04.097>.
9. M. Gao and R. P. Wei, Grain boundary niobium carbides in Inconel 718. *Scripta Materialia* **6462**, (97), 1843–1849 (1997).
10. J. González, L. B. Peral, C. Colombo, and I. F. Pariente, A study on the microstructural evolution of a low alloy steel by different shot peening treatments. *Metals* **8**, (3), 187. <https://doi.org/10.3390/met8030187>
11. A. Zammit, M. Mhaede, M. Grech, S. Abela, and L. Wagner, Influence of shot peening on the fatigue life of Cu–Ni austempered ductile iron. *Materials Science and Engineering A* **545**, 78–85 (2012). <https://doi.org/10.1016/j.msea.2012.02.092>.
12. J. González, L. B. Peral, A. Zafra, and I. Fernández-Pariente, Influence of shot peening treatment in erosion wear behavior of high chromium white cast iron. *Metals* **9**, (9), 933. <https://doi.org/10.3390/met9090933>.
13. E. Real, C. Rodríguez, F. J. Belzunce, P. Sanjurjo, A. F. Canteli, and I. Fernández-Pariente, Fatigue behaviour of duplex stainless steel reinforcing bars subjected to shot peening. *Fatigue and Fracture of Engineering Materials and Structures* **32**, (7), 567–572 (2009). <https://doi.org/10.1111/j.1460-2695.2009.01360.x>.
14. T. Klotz, D. Delbergue, P. Bocher, M. Lévesque, and M. Brochu, Surface characteristics and fatigue behavior of shot peened Inconel 718. *International Journal of Fatigue* **110**, 10–21 (2018). <https://doi.org/10.1016/j.ijfatigue.2018.01.005>.
15. P. S. Prevéry, The effect of cold work on the thermal stability of residual compression in surface enhanced IN718. *ASM Proceedings: Heat Treating* **1**, 426–434 (2000).
16. J. Hoffmeister, V. Schulze, A. Wanner, R. Hessert, and G. Koenig, Thermal Relaxation of residual Stresses induced by Shot Peening in IN718, 10th International Conference on Shot Peening (ICSP-10) (2008) 1–6.
17. J. Smialek, *Superalloys II*, (1987), 2016.
18. G. R. Wallwork, The oxidation of alloys. *Rep. Prog. Phys.*
19. R. Molins, G. Hochstetter, J. C. Chassigne, and E. Andrieu, Oxidation effects on the fatigue crack growth behaviour of alloy 718 at high temperature. *Acta Materialia* **45**, (2), 663–674 (1997). [https://doi.org/10.1016/S1359-6454\(96\)00192-9](https://doi.org/10.1016/S1359-6454(96)00192-9).
20. D. Serafin, W. J. Nowak, and B. Wierzba, The effect of surface preparation on high temperature oxidation of Ni, Cu and Ni–Cu alloy. *Applied Surface Science* **476**, 442–451 (2019). <https://doi.org/10.1016/j.apsusc.2019.01.122>.
21. S. Cruchley, M. P. Taylor, R. Ding, H. E. Evans, D. J. Child, and M. C. Hardy, Comparison of chromia growth kinetics in a Ni-based superalloy, with and without shot-peening. *Corrosion Science* **100**, 242–252 (2015). <https://doi.org/10.1016/j.corsci.2015.07.033>.
22. W. J. Nowak and B. Wierzba, Effect of surface treatment on high-temperature oxidation behavior of IN 713C. *Journal of Materials Engineering and Performance* **27**, (10), 5280–5290 (2018). <https://doi.org/10.1007/s11665-018-3621-2>.
23. Z. G. Zhang, P. Y. Hou, F. Gesmundo, and N. Y., Effect of surface roughness on the development of protective α_2 or α_3 on Fe-10Al (at.) alloys containing 0–10 at. cr. *Applied Surface Science* **253** (2), 881–888 (2006). <https://doi.org/10.1016/j.apsusc.2006.01.027>.
24. S. Cruchley, H. Evans, and M. Taylor, An overview of the oxidation of Ni-based superalloys for turbine disc applications: surface condition, applied load and mechanical performance. *Materials at High Temperatures* **33**, (4–5), (465–475 (2016). <https://doi.org/10.1080/09603409.2016.1171952>.
25. W. C. Liu, Z. L. Chen, and M. Yao, Effect of cold rolling on the precipitation behavior of δ phase in INCONEL718. *Metallurgical and Materials Transactions A: Physical Metallurgy and Materials Science* **30**, (1), 31–40 (1999). <https://doi.org/10.1007/s11661-999-0193-7>.

26. Y. Mei, Y. Liu, C. Liu, C. Li, L. Yu, Q. Guo, and H. Li, Effects of cold rolling on the precipitation kinetics and the morphology evolution of intermediate phases in Inconel 718 alloy. *Journal of Alloys and Compounds* **649**, 949–960 (2015). <https://doi.org/10.1016/j.jallcom.2015.07.149>.
27. Zirshot technical data sheet (2012) <https://www.zirpro.com>.
28. D. Kirk, and M. Abyaneh, Theoretical basis of shot peening coverage control. *Shot Peener (USA)* **9** (2), 28–30 (1995).
29. M. E. Fitzpatrick, A. Fry, P. Holdway, F. a. Kandil, J. Shackleton, and L. Suominen, Measurement Good Practice Guide No. 52. Determination of Residual Stresses by X-ray Diffraction, Measurement Good Practice Guide (2) **74** (2005).
30. M. Moore and W. Evans, Correction for stress layers in X-ray diffraction residual stress analysis. *SAE Transactions* **66**, 340–345 (1958).
31. L. B. Peral, A. Quintero, A. T. Vielma, M. F. Barbés, and I. Fernández-Pariente, TEM evaluation of steel nanocrystalline surfaces obtained by severe shot peening. *Surface and Coatings Technology* **418** 127238 (2021). <https://doi.org/10.1016/j.surfcoat.2021.127238>.
32. L. B. Peral, P. Ebrahimzadeh, A. Gutiérrez, and I. Fernández-Pariente, Effect of tempering temperature and grain refinement induced by severe shot peening on the corrosion behavior of a low alloy steel. *Journal of Electroanalytical Chemistry* **932**, 117207 (2023). <https://doi.org/10.1016/j.jelechem.2023.117207>.
33. K. Dai and L. Shaw, Comparison between shot peening and surface nanocrystallization and hardening processes. *Materials Science and Engineering A* **463**, (1–2), 46–53 (2007). <https://doi.org/10.1016/j.msea.2006.07.159>.
34. Y. K. Gao, M. Yao, and J. K. Li, An analysis of residual stress fields caused by shot peening. *Metallurgical and Materials Transactions A: Physical Metallurgy and Materials Science* **33**, (6), 1775–1778 (2002). <https://doi.org/10.1007/s11661-002-0186-2>.
35. G. A. Greene and C. C. Finfrock, Oxidation of inconel 718 in air at high temperatures. *Oxidation of Metals* **55**, (5–6), 505–521 (2001). <https://doi.org/10.1023/a:1010359815550>.
36. K. A. Al-Hatab, M. A. Al-Bukhaiti, U. Krupp, and M. Kantehm, Cyclic oxidation behavior of in 718 superalloy in air at high temperatures. *Oxidation of Metals* **75**, (3–4), 209–228 (2011). <https://doi.org/10.1007/s11085-010-9230-6>.
37. D. Cai, P. Nie, J. Shan, W. Liu, Y. Gao, and M. Yao, Precipitation and residual stress relaxation kinetics in shot-peened inconel 718. *Journal of Materials Engineering and Performance* **15**, (5), 614–617 (2006). <https://doi.org/10.1361/105994906X124613>.
38. L. B. Peral, and I. Fernández-Pariente, TEM evaluation of steel nanocrystalline surfaces obtained by severe shot peening. *Surface and Coatings Technology* **418**, 127238 (2021).
39. H. Qin, Z. Bi, H. Yu, G. Feng, J. Du, and J. Zhang, Influence of stress on γ'' precipitation behavior in inconel 718 during aging. *Journal of Alloys and Compounds* **740**, 997–1006 (2018). <https://doi.org/10.1016/j.jallcom.2018.01.030>.

Publisher's Note Springer Nature remains neutral with regard to jurisdictional claims in published maps and institutional affiliations.